

A Family of Self-Dual Quasicrystals with Critical Phases

Wenzhi Wang,¹ Wei Yi,^{1,2,3,4,5,*} and Tianyu Li^{6,7,†}

¹Laboratory of Quantum Information, University of Science and Technology of China, Hefei 230026, China

²Anhui Province Key Laboratory of Quantum Network,
University of Science and Technology of China, Hefei 230026, China

³CAS Center For Excellence in Quantum Information and Quantum Physics, Hefei 230026, China

⁴Hefei National Laboratory, University of Science and Technology of China, Hefei 230088, China

⁵Anhui Center for Fundamental Sciences in Theoretical Physics,
University of Science and Technology of China, Hefei 230026, China

⁶Key Laboratory of Atomic and Subatomic Structure and Quantum Control (Ministry of Education),
Guangdong Basic Research Center of Excellence for Structure and Fundamental Interactions of Matter,
School of Physics, South China Normal University, Guangzhou 510006, China

⁷Guangdong Provincial Key Laboratory of Quantum Engineering and Quantum Materials,
Guangdong-Hong Kong Joint Laboratory of Quantum Matter,
Frontier Research Institute for Physics, South China Normal University, Guangzhou 510006, China

We propose a general framework for constructing self-dual one-dimensional quasiperiodic lattice models with arbitrary-range hoppings and multifractal behaviors. Our framework generates a broad spectrum of quasicrystals, ranging from the off-diagonal Aubry-André-Harper models on one end, to those with long-range power-law hoppings on another. Focusing on models with off-diagonal quasiperiodic hoppings with power-law decay, we exploit the fact that, when the self-dual condition is satisfied, the system must be in the critical state with multifractal properties. This enables the engineering of models with competing extended, critical, and localized phases, with rich mobility edges in between. As an outstanding example, we show that a limiting case of our family of self-dual quasicrystals can be implemented using Rydberg-atom arrays. Our work offers a systematic route toward self-duality and critical phases, and would facilitate their experimental simulation.

Introduction.— Anderson localization is a fundamental quantum phenomenon in which disorder leads to the exponential localization of eigenstates, thereby inhibiting wave diffusion [1–6]. The associated localization-delocalization transition generally depends on the spatial dimensions, for instance, an infinitesimally weak disorder is sufficient to induce Anderson localization in one dimension [7–9]. But Anderson localization also arises in quasiperiodic models, where, in a one dimensional quasicrystal for instance, the localization only occurs beyond a critical threshold of the quasiperiodic potential. This is exemplified by the well-known Aubry-André-Harper (AAH) model [10], characterized by the eigen equation $t(\psi_{n+1} + \psi_{n-1}) + V \cos(2\pi\tau n)\psi_n = E\psi_n$, where ψ_n is the wavefunction component on site n , t is the nearest-neighbor hopping strength, V is the amplitude of the quasiperiodic potential, τ is an irrational number, and E is the eigenenergy. Crucially, the AAH model exhibits self-duality, such that it Fourier-transforms onto itself but with switched parameters $V \leftrightarrow 2t$. The self-dual point $V = 2t$ thus marks a sharp transition between the extended (for $V < 2t$) and localized (for $V > 2t$) phases. Remarkably, at the self-dual point, the system becomes critically localized [11–21].

Further engineering of the AAH model can have two important consequences. First, with the addition of off-diagonal quasiperiodic potentials, the critical point can be expanded into a critical phase occupying a broad region on the phase diagram. These critical states are extended yet nonergodic, exhibiting unique spectral statis-

tics [22–24], multifractal properties [25–27], and unconventional dynamics [28–30]. Second, by introducing long-range hopping terms [31] or fine-tuned on-site quasiperiodic potentials [32], mobility edges emerge in the eigenspectrum, where critical energies separate extended and localized states [3, 5, 31–36]. These possibilities have sparked widespread interest in quasiperiodic systems, including theoretical studies on periodically (or quasiperiodically) driven systems [37–42] and non-Hermitian quasicrystals [43–53], as well as experimental implementations using ultracold atoms [54–64], photonic crystals [65–72], optical cavities [73, 74], and superconducting circuits [75, 76]. Despite these activities, the general mechanisms responsible for the emergence of critical states remain an open question, and the coexistence (in the same phase diagram) of extended, critical, and localized phases has so far been observed only in a handful of fine-tuned models. While it is tempting to address these issues from the perspective of self-duality, only a limited number of quasiperiodic models are known to be self-dual.

In this work, we propose a general framework for constructing self-dual one-dimensional quasiperiodic models with arbitrary-range hopping and critical behaviors. Similar to the AAH example, with our scheme, a model constructed with the parameters (a, b) is dual to the same model but parameterized by (b, a) . This naturally leads to the self-dual condition $a = b$, where the system must be in the critical state. The family of quasicrystals so generated spans a wide spectrum, with the

(generalized) AAH models on one end, and those with long-range hoppings on another. Inspired by the recent experimental progress of Rydberg-atom arrays, we focus on models exhibiting off-diagonal quasiperiodic hoppings with power-law decay. Consistent with our expectation, the system is in the critical phase close to the self-dual point. The overall phase diagram is symmetric with respect to the self-dual condition $a = b$, featuring rich mobility edges in between the extended, critical, and localized phases. We then demonstrate that the model parameterized by $(3, +\infty)$, which features both extended and critical phases, can be experimentally realized using Rydberg atoms with dipole-dipole interactions. Our work provides a general scheme for engineering self-dual quasicrystals, as well as a route toward critical phases from self-duality considerations.

Self-dual quasicrystals.— We consider a family of one-dimensional tight-binding models

$$\hat{H}(a, b) = \sum_{m \neq n} \hat{b}_m^\dagger \hat{b}_n f_{|m-n|}(a) F_{m+n}(b), \quad (1)$$

where \hat{b}_n^\dagger (\hat{b}_n) are the creation (annihilation) operators on site n . The hopping coefficients are determined by the product of two functions, $f_{|m-n|}(a)$ and $F_{m+n}(b)$, which depend on the site index and the real parameters a and b . Furthermore, we require that the two functions be related according to

$$F_x(a) = \sum_{s=1}^{+\infty} f_s(a) \cos(\tau s \pi x), \quad (2)$$

where the irrational number $\tau = (\sqrt{5} - 1)/2$. Performing the dual transformation

$$\tilde{b}_k = \frac{1}{\sqrt{N}} \sum_{m=1}^N e^{-2i\pi\tau mk} \hat{b}_m, \quad (3)$$

where N represents the total number of sites, the Hamiltonian in the dual space reads [77]

$$\hat{H}(a, b) = \sum_{k \neq l} \tilde{b}_k^\dagger \tilde{b}_l f_{|k-l|}(b) F_{k+l}(a). \quad (4)$$

Equations (1) and (4) establish that $\hat{H}(a, b)$ and $\hat{H}(b, a)$ are dual to each other, such that $a = b$ defines the self-dual condition. It follows that, if the j th eigenstate of $\hat{H}(a, b)$, denoted as $\psi^{(j)}$, is localized, then the j th eigenstate of $\hat{H}(b, a)$, denoted as $\tilde{\psi}^{(j)}$, must be extended, and vice versa. Furthermore, if $\psi^{(j)}$ is critical, then $\tilde{\psi}^{(j)}$ is also critical, such that all eigenstates of $\hat{H}(a, a)$ are critical, being at the self-dual point $a = b$. Note that, in the following, we index the eigenstates according to their eigenenergies in ascending order.

Here two remarks are in order. First, Hamiltonian $\hat{H}(a, b)$ is determined by the functions $\{f_s(a)\}_{s=1,2,\dots,+\infty}$,

which are arbitrary, and subject only to the constraint that the summation in Eq. (2) should converge. Second, such a flexibility allows us to construct a broad class of self-dual quasicrystals with multifractal properties [77].

As a notable special case, we set $f_1(a) = a$, and $f_s(a) = 0$ for $s \neq 1$. We then have

$$F_x(a) = a \cos(\tau \pi x), \quad (5)$$

which leads to the Hamiltonian

$$\hat{H}(a, b) = \sum_n ab \cos[\tau \pi (2n + 1)] (\hat{b}_{n+1}^\dagger \hat{b}_n + \hat{b}_n^\dagger \hat{b}_{n+1}). \quad (6)$$

This is the well-studied off-diagonal AAH model [53, 78]. Since Eq. (6) remains invariant under the dual transformation, with $\hat{H}(a, b) = \hat{H}(b, a)$, all eigenstates of the off-diagonal AAH model are critical. Note that the conventional AAH model can also be generated based on our construction [77].

Quasicrystals with power-law hoppings.— Inspired by the recent progress in Rydberg-atom arrays with long-range interactions, we now focus on a class of quasiperiodic models with power-law hopping terms. Specifically, we consider $f_s(a) = \frac{1}{s^a}$ for $s \leq d$, and $f_s(a) = 0$ for $s > d$. In this case, we have

$$F_x(a) = \sum_{s=1}^d \frac{1}{s^a} \cos(\tau s \pi x), \quad (7)$$

and the corresponding Hamiltonian is

$$\hat{H}_p(a, b) = \sum_{1 \leq |m-n| \leq d} \hat{b}_m^\dagger \hat{b}_n \frac{1}{|m-n|^a} \sum_{s=1}^d \frac{1}{s^b} \cos[\tau s \pi (m+n)], \quad (8)$$

where d denotes the maximum hopping range, while a and b respectively characterize the exponent of the power-law decay in hopping, and the amplitude modulation.

To corroborate the self-duality and localization properties of the model, we study the fractal dimension (FD) of $\hat{H}_p(a, b)$. The fractal dimension is given by

$$\text{FD} = -\frac{\ln(\text{IPR}_j)}{\ln(N)}, \quad (9)$$

where the inverse participation ratio of the j th eigenstate is defined as $\text{IPR}_j = \sum_n |\psi_n^{(j)}|^4$, with $\psi_n^{(j)}$ indicating the component on site n of the j th eigenstate. In the thermodynamic limit, FD approaches 1 for extended states, and 0 for localized states, while $0 < \text{FD} < 1$ signifies the critical states [21, 79].

As a convenient sampling of the parameter space, we impose the constraint $a + b = 4$, such that the self-dual condition is satisfied for $a = 2$. In Fig. 1(a)(b), we show the computed FD as functions of a and the eigenstate

index j/N for different hopping ranges d . The resulting phase diagram exhibits a rich structure, featuring all three phases: the extended (red), the critical (green), and the localized (blue). Consistent with the self-dual properties of the model, the phase diagram is symmetric: regions of the extended (localized) phase to the left of $a = 2$ are symmetric to those of the localized (extended) phase to the right, while regions of the critical phase are symmetric with respect to $a = 2$. With increasing hopping range d , the stability region of the critical phase shrinks and becomes fragmented.

In Fig. 1(c), we show the fractal dimension as a function of the eigenstate index j/N for different system sizes. In the localized regions (marked I and IV), FD tends toward zero with increasing system size, while in the extended region (marked III), FD increases toward unity. In contrast, in the critical region (marked II), FD remains between 0 and 1, showing minimal dependence on the system size.

Alternatively, the three phases can be distinguished by analyzing the level statistics. Denoting the ordered eigenenergies as $\{E_j\}_{j=1,2,\dots,N}$, we define the even-odd eigen-level spacing as $s_{2j}^{e-o} = E_{2j} - E_{2j-1}$, and the odd-even eigen-level spacing $s_{2j+1}^{o-e} = E_{2j+1} - E_{2j}$ [11, 41]. In the extended phase, the spectrum is nearly doubly degenerate, leading to $s_{2j+1}^{o-e} \sim 0$, so that a noticeable gap exists between s_{2j}^{e-o} and s_{2j+1}^{o-e} . In the localized phase, such degeneracies vanish, and the numerically calculated gap sharply decreases in magnitude. In the critical phase, both s_{2j}^{e-o} and s_{2j+1}^{o-e} exhibit strongly scattered distributions, indicative of its multifractal properties [11]. These expected features are clearly visible in Fig. 1(d), with the phase boundaries consistent with those in Fig. 1(a)(c).

Next, we consider a particular limiting case of Eq. (8)

$$\hat{H}_p(a, +\infty) = \sum_{1 \leq |m-n| \leq d} \hat{b}_m^\dagger \hat{b}_n \frac{\cos[\tau\pi(m+n)]}{|m-n|^a}, \quad (10)$$

whose dual is given by

$$\hat{H}_p(+\infty, a) = \sum_m (\hat{b}_m^\dagger \hat{b}_{m+1} + \hat{b}_{m+1}^\dagger \hat{b}_m) \sum_{s=1}^d \frac{\cos[\tau s \pi(2m+1)]}{s^a}. \quad (11)$$

Note that $\hat{H}(a, +\infty)$ features long-range hoppings with a single quasiperiodicity, whereas its dual $\hat{H}(+\infty, a)$ involves only nearest-neighbor hopping, modulated by a sum of quasiperiodic components.

In Fig. 2(a)(b), we show the fractal dimensions of the eigenstates of $\hat{H}(a, +\infty)$ and $\hat{H}(+\infty, a)$, respectively. While $\hat{H}(a, +\infty)$ possesses only extended and critical phases, its dual $\hat{H}(+\infty, a)$ supports localized and critical phases. In either case, the phase diagram is symmetric with respect to $j/N = 1/2$, which originates from a spectral symmetry: for each eigenvalue E , its opposite eigenvalue $-E$ also exists in the spectrum, with both eigenstates featuring the same spatial localization since

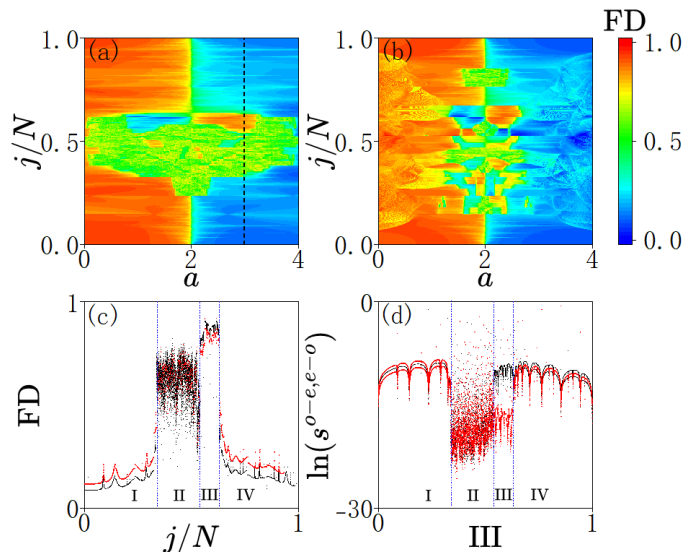


FIG. 1. Fractal dimension FD of $\hat{H}_p(a, 4-a)$ for (a) $d = 2$, and (b) $d = 10$. (c) The fractal dimension as a function of the eigenstate index j/N , with fixed $a = 3$ [the vertical black dashed line in (a)], for $N = 2584$ (red dots) and $N = 46368$ (black dots), respectively. (d) The even-odd eigen-level spacings s_{2j}^{e-o} (black dots) and s_{2j+1}^{o-e} (red dots) as functions of j/N for $N = 28657$. The vertical blue dashed lines in (c) and (d) indicate the positions of the mobility edge, separating four distinct regions corresponding to the localized (I, IV), critical (II), and extended (III) phases. We take $N = 2584$ in (a)(b), and impose the periodic boundary condition for all calculations.

they differ only by a sign reversal on odd (or even) lattice sites [77]. Furthermore, regions with mobility edges that are constant in $j/N = P_{1,2,3,4}$ can be identified, with $P_1 = 1 - \tau$, $P_2 = 20\tau - 12$, $P_3 = 7\tau - 4$, and $P_4 = 2\tau - 1$, all independent of the system size. Note that, although the positions of these mobility edges remain unchanged in terms of the eigenstate index j/N within each region in Fig. 2, their corresponding eigenenergies vary with a . These mobility edges separate the extended (red) or localized (blue) phases from the critical phase (green). To better identify these phases, we compute the standard deviation of the fractal dimension [20], defined as $\sigma^2(FD) = \langle (FD)^2 \rangle - \langle FD \rangle^2$, where the average is taken over eigenstates in a specified interval. Figure 2(c) shows $\sigma^2(FD)$ as a function of a for both $\hat{H}(a, +\infty)$ (black dots) and $\hat{H}(+\infty, a)$ (red dots), with the average taken over the interval $j/N \in [0, P_4]$. As expected, $\sigma^2(FD)$ exhibits distinct behaviors in different phases: it tends toward zero in the localized region, remains finite in the extended region, and takes intermediate values in the critical region.

Lyapunov exponents (LEs) offer another useful diagnostic for localization. For an eigenstate with energy E , the LE is defined as [18, 19]

$$\gamma(E) = \lim_{N \rightarrow \infty} \frac{1}{N} \ln \|\Pi_{n=1}^N T_n\|, \quad (12)$$

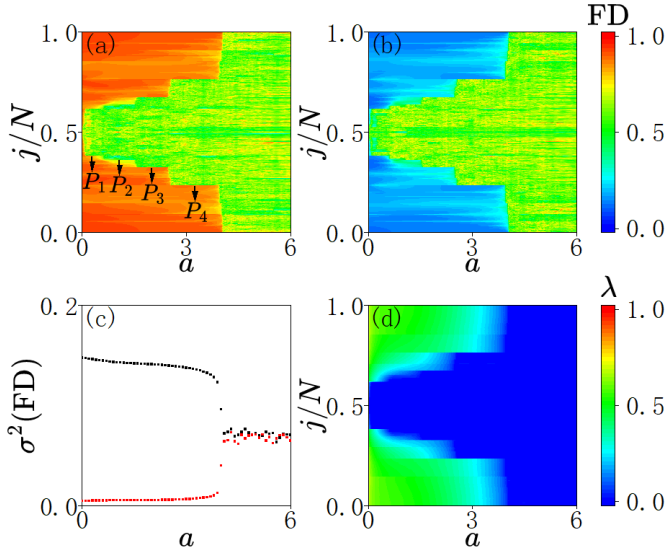


FIG. 2. Fractal dimensions for different eigenstates with $d = 2$ for (a) $\hat{H}_p(a, +\infty)$ and (b) $\hat{H}_p(+\infty, a)$. Four characteristic regions with step-wise mobility edges in j/N can be identified, labeled by $j/N = P_{1,2,3,4}$. (c) The standard deviation of FD, $\sigma^2(\text{FD})$, as a function of a for $\hat{H}(a, +\infty)$ (black dots) and $\hat{H}(+\infty, a)$ (red dots), with the average taken over the eigenstates in the interval $j/N \in [0, P_4]$. (d) The Lyapunov exponent as a function of a and j/N . For all calculations, we take $N = 2584$, and impose the periodic boundary condition.

where $\|\cdot\|$ denotes the matrix norm, and the transfer matrix T_n is given by

$$T_n = \begin{pmatrix} E & -t_{n-1} \\ t_n & 0 \end{pmatrix}, \quad (13)$$

with $t_n = \sum_{s=1}^d \frac{\cos[\tau s \pi (2n+1)]}{s^a}$. Here the calculation is feasible since the transfer matrices are easily accessible for $\hat{H}_p(a, +\infty)$ and $\hat{H}_p(+\infty, a)$, which is not generally the case for $\hat{H}_p(a, b)$. In Fig. 2(d), we show the calculated LE as a function a and j/N , the results match excellently with the phase diagram in Fig. 2(b). Specifically, for critical states, the LE vanishes ($\gamma = 0$), while for localized states, it remains finite [19].

Experimental realization using Rydberg atoms.— The dipole-dipole interactions in Rydberg atoms dictate a $1/r^3$ long-range power-law decay. Based on such an observation, we illustrate below that the model in Eq. (10) can be experimentally realized in a Rydberg-atom array for $a = 3$.

Consider a one-dimensional array of ^{87}Rb atoms for instance. As illustrated in Fig. 3(a), the internal-state space of the atom on the n th site consists of the Rydberg states $|60S_{1/2}, m_j = 1/2\rangle$, denoted as $|0\rangle_n$, as well as $|60P_{3/2}, m_j = 3/2\rangle$ and $|60P_{3/2}, m_j = -1/2\rangle$, denoted as $|+\rangle_n$ and $|-\rangle_n$, respectively. A site-dependent energy splitting of $2\Delta_n$ is imposed between the states $|+\rangle_n$ and

$|-\rangle_n$, which can be induced by a magnetic-field gradient. These two states are further coupled by a site-dependent microwave field with Rabi frequency Ω_n . By moving to the eigenbasis of the microwave-dressed states [77], the internal degrees of freedom of the atom on the n th site are labeled $\{|0\rangle_n, |\xi_{\pm}\rangle_n\}$, as shown in Fig. 3(b).

Assuming a constant $\Delta_n^2 + \Omega_n^2$, we perform the rotating-wave approximation in an appropriate rotating frame, arriving at the Hamiltonian [77, 80]

$$\hat{H}_I = \sum_{m \neq n} J_{\xi_+, mn} \hat{b}_{\xi_+, m}^\dagger \hat{b}_{\xi_+, n} + J_{\xi_-, mn} \hat{b}_{\xi_-, m}^\dagger \hat{b}_{\xi_-, n}, \quad (14)$$

where $J_{\xi_+, mn}$ and $J_{\xi_-, mn}$ are the corresponding coupling coefficients, and the creation operators are $\hat{b}_{\xi_+, n}^\dagger = |\xi_+\rangle_n \langle 0|_n$ and $\hat{b}_{\xi_-, n}^\dagger = |\xi_-\rangle_n \langle 0|_n$.

Further requiring that the energy splittings between the microwave-dressed basis be much larger than the dipole interaction energy [77], we focus on the case where only a single excited state $|\xi_+\rangle$ is present in the system. Then, the Hamiltonian simplifies to

$$\hat{H}_I = \sum_{m \neq n} J_{\xi_+, mn} \hat{b}_{\xi_+, m}^\dagger \hat{b}_{\xi_+, n}, \quad (15)$$

where the coupling coefficients are

$$J_{\xi_+, mn} = \frac{1}{|m-n|^3} \left(\cos \frac{\alpha_m - \alpha_n}{2} Y_{20} + \sqrt{6} \cos \frac{\alpha_m}{2} \sin \frac{\alpha_n}{2} Y_{2-2} + \sqrt{6} \cos \frac{\alpha_n}{2} \sin \frac{\alpha_m}{2} Y_{22} \right). \quad (16)$$

Here $\cos \alpha_n = \frac{\Delta_n}{\sqrt{\Delta_n^2 + \Omega_n^2}}$, $\sin \alpha_n = \frac{\Omega_n}{\sqrt{\Delta_n^2 + \Omega_n^2}}$, and $\{Y_{20}, Y_{2\pm 2}\}$ are the spherical harmonics. We set $Y_{20} = 0$ and $Y_{2-2} = Y_{22}$ by adjusting the relative orientation between the Rydberg-atom array and the spherical coordinate. By further setting appropriate values of Δ_n and Ω_n , such that $\alpha_n = 2\pi\tau n + \frac{\pi}{2}$, the Hamiltonian reduces to

$$\hat{H}_{\xi_{\pm}} = A \sum_{m \neq n} \frac{\cos[\pi\tau(m+n)]}{|m-n|^3} \hat{b}_{\xi_+, m}^\dagger \hat{b}_{\xi_+, n}, \quad (17)$$

which recovers Eq. (10). Here the pre-factor A is proportional to the dipolar interaction energy between adjacent atoms.

In Fig. 3(c)(d), we show the fractal dimension of different eigenstates of the Hamiltonian (17) and its dual model, with varying interaction range d . Notably, for Eq. (17) [see Fig. 3(c)], two mobility edges separate the extended and critical phases, and they remain unchanged in terms of the eigenstate index j/N across all values of d (although their corresponding energies should vary with d). For its dual model, two mobility edges similarly separate the localized and critical phases, which also remain unchanged in terms of j/N for all values of d [see

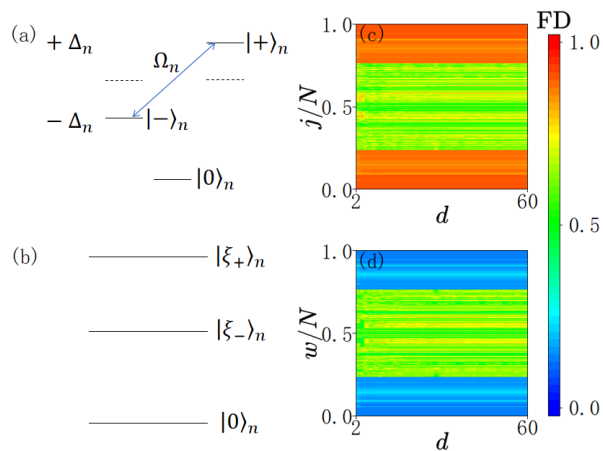


FIG. 3. (a) Level scheme of the microwave-dressed Rydberg states of the n th atom in the one-dimensional array. Here $2\Delta_n$ is the site-dependent energy splitting between the Rydberg states $|+\rangle_n$ and $|-\rangle_n$, Ω_n is the Rabi frequency of the coupling between $|+\rangle_n$ and $|-\rangle_n$. (b) Level scheme for the microwave-dressed basis of the n th atom. (c)(d) Fractal dimension FD of different eigenstates with varying interaction (hopping) range d for (c) $H(3, +\infty)$ and (d) $H(+\infty, 3)$, respectively. The two mobility edges are located at $j/N = 2 - 2\tau$ and $2\tau - 1$, respectively. For all calculations, the system size is $N = 2584$ and we impose the periodic boundary condition.

Fig. 3(d)]. Experimentally, the different phases can be identified by investigating the propagation of a single localized excitation [30].

Discussions.— We have developed a general framework for engineering self-dual one-dimensional quasicrystals. The scheme enables the construction of a family of quasiperiodic models with critical phases in a rich phase diagram. Our work offers a systematic route toward self-duality, and, by linking self-duality with critical states, also provides a practical access to the latter. For instance, given the generality of our scheme, it is straightforward to construct self-dual models for Rydberg-atom arrays with long-range van der Waals interactions that feature $1/r^6$ power-law decay. For future studies, it would be interesting to extend the framework to higher dimensions. It would also be desirable to engineer energy-dependent self-dual conditions that yield analytically solvable mobility edges.

* wyiz@ustc.edu.cn

† tianyuli@m.scnu.edu.cn

- [1] P. W. Anderson, Absence of diffusion in certain random lattices, Phys. Rev. **109**, 1492 (1958).
 [2] P. A. Lee and T. V. Ramakrishnan, Disordered electronic systems, Rev. Mod. Phys. **57**, 287 (1985).
 [3] A. Lagendijk, B. Tiggelen, and D. S. Wiersma, Fifty years of Anderson localization, Phys. Today **62**(8), 24

- (2009).
 [4] B. Kramer and A. MacKinnon, Localization: theory and experiment, Rep. Prog. Phys. **56**, 1469 (1993).
 [5] F. Evers and A. D. Mirlin, Anderson transitions, Rev. Mod. Phys. **80**, 1355 (2008).
 [6] A. Lagendijk, B. Tiggelen, and D. S. Wiersma, Fifty years of Anderson localization, Phys. Today **62**, 24 (2009).
 [7] D. Thouless, Electrons in disordered systems and the theory of localization, Physics Reports **13**(3), 93 (1974).
 [8] E. Abrahams, P. W. Anderson, D. C. Licciardello, and T. V. Ramakrishnan, Scaling theory of localization: absence of quantum diffusion in two dimensions, Phys. Rev. Lett. **42**, 673 (1979).
 [9] B. Hetényi, S. Parlak, and M. Yahyavi, Scaling and renormalization in the modern theory of polarization: Application to disordered systems, Phys. Rev. B **104**, 214207(2021).
 [10] S. Aubry and G. Andre, Analyticity breaking and Anderson localization in incommensurate lattices, Ann. Israel Phys. Soc. **3**, 133 (1980).
 [11] X. Deng, S. Ray, S. Sinha, G.V. Shlyapnikov, and L. Santos, One-Dimensional Quasicrystals with Power-Law Hopping. Phys. Rev. Lett. **123**, 025301(2019).
 [12] H. Li, Y.-Y Wang, Y.-H Shi, K. Huang, X. Song, G.-H Liang, Z.-Y Mei, B. Zhou, H. Zhang, J.-C Zhang, S. Chen, S.-P. Zhao, Y. Tian, Z.-Y Yang, Z. Xiang, K. Xu, D. Zheng, and H. Fan, Observation of critical phase transition in a generalized Aubry-André-Harper model with superconducting circuits, npj Quantum Inf. **9**, 40 (2023).
 [13] Y. Hatsugai and M. Kohmoto, Energy spectrum and the quantum Hall effect on the square lattice with nextnearest-neighbor hopping, Phys. Rev. B **42**, 8282 (1990).
 [14] J. H. Han, D. J. Thouless, H. Hiramoto, and M. Kohmoto, Critical and bicritical properties of Harper's equation with next-nearest-neighbor coupling, Phys. Rev. B **50**, 11365 (1994).
 [15] Y. Takada, K. Ino, and M. Yamanaka, Statistics of spectra for critical quantum chaos in one-dimensional quasiperiodic systems, Phys. Rev. E **70**, 066203 (2004).
 [16] F. Liu, S. Ghosh, and Y. D. Chong, Localization and adiabatic pumping in a generalized Aubry-André-Harper model, Phys. Rev. B **91**, 014108 (2015).
 [17] J. Wang, X.-J. Liu, X. Gao, and H. Hu, Phase diagram of a non-Abelian Aubry-André-Harper model with p-wave superfluidity, Phys. Rev. B **93**, 104504 (2016).
 [18] Shan-Zhong Li, Yi-Cai Zhang, Yucheng Wang, Shan-chao Zhang, Shi-Liang Zhu, Zhi Li, Multifractal-enriched mobility edges and emergent quantum phases in one-dimensional exactly solvable lattice models. arXiv:2501.07866(2025).
 [19] T. Liu, and X. Xu, Predicted critical state based on invariance of the Lyapunov exponent in dual spaces, Chin. Phys. Lett. **41** 017102 (2024).
 [20] S. Gopalakrishnan, Self-dual quasiperiodic systems with power-law hopping, Phys. Rev. B **96**, 054202 (2017).
 [21] X.-C. Zhou, Y. Wang, T.-F. J. Poon, Q. Zhou and X.-J. Liu, Exact New Mobility Edges between Critical and Localized States. Phys. Rev. Lett. **131**, 176401(2023).
 [22] T. Geisel, R. Ketzmerick, and G. Petschel, New class of level statistics in quantum systems with unbounded diffusion, Phys. Rev. Lett. **66**, 1651 (1991).
 [23] K. Machida and M. Fujita, Quantum energy spectra and one-dimensional quasiperiodic systems, Phys. Rev. B **34**,

- 7367 (1986).
- [24] C. L. Bertrand and A. M. García-García, Anomalous Thouless energy and critical statistics on the metallic side of the many-body localization transition, *Phys. Rev. B* **94**, 144201 (2016).
- [25] T. C. Halsey, M. H. Jensen, L. P. Kadanoff, I. Procaccia, and B. I. Shraiman, Fractal measures and their singularities: The characterization of strange sets, *Phys. Rev. A* **33**, 1141(1986).
- [26] A. D. Mirlin, Y. V. Fyodorov, A. Mildenberger, and F. Evers, Exact relations between multifractal exponents at the Anderson transition, *Phys. Rev. Lett.* **97**, 046803 (2006).
- [27] R. Dubertrand, I. García-Mata, B. Georgeot, O. Giraud, G. Lemarie, and J. Martin, Two scenarios for quantum multifractality breakdown, *Phys. Rev. Lett.* **112**, 234101 (2014).
- [28] H. Hiramoto and S. Abe, Dynamics of an electron in quasiperiodic systems. II. Harper's model, *J. Phys. Soc. Jpn.* **57**, 1365 (1988).
- [29] R. Ketzmerick, K. Kruse, S. Kraut, and T. Geisel, What determines the spreading of a wave packet?, *Phys. Rev. Lett.* **79**, 1959 (1997).
- [30] M. Larcher, F. Dalfovo, and M. Modugno, Effects of interaction on the diffusion of atomic matter waves in one-dimensional quasiperiodic potentials, *Phys. Rev. A* **80**, 053606 (2009).
- [31] J. Biddle and S. Das Sarma, Predicted Mobility Edges in One-Dimensional Incommensurate Optical Lattices: An Exactly Solvable Model of Anderson Localization, *Phys. Rev. Lett.* **104**, 070601 (2010).
- [32] S. Ganeshan, J. H. Pixley, and S. Das Sarma, Nearest Neighbor Tight Binding Models with An Exact Mobility Edge in One Dimension, *Phys. Rev. Lett.* **114**, 146601(2015).
- [33] Y. Wang, X. Xia, L. Zhang, H. Yao, S. Chen, J. You, Q. Zhou, and X.-J. Liu, One Dimensional Quasiperiodic Mosaic Lattice with Exact Mobility Edges, *Phys. Rev. Lett.* **125**, 196604(2020).
- [34] J. Biddle, D. J. Priour, Jr., B. Wang, and S. Das Sarma, Localization in one-dimensional lattices with non-neighbor hopping: Generalized Anderson and Aubry-Andre models, *Phys. Rev. B* **83**, 075105 (2011).
- [35] X. Li, and S. Das Sarma, Mobility edges and intermediate phase in one-dimensional incommensurate lattice potentials, *Phys. Rev. B* **101**, 064203 (2020).
- [36] Hai-Tao Hu, Xiaoshui Lin, Ai-Min Guo, Zijin Lin, Ming Gong, Hidden self-duality in quasiperiodic network models. arXiv:2411.06843(2024).
- [37] T. Cadez, R. Mondaini, and P. D. Sacramento, Dynamical localization and the effects of aperiodicity in Floquet systems, *Phys. Rev. B* **96**, 144301 (2017).
- [38] S. Roy, I. M. Khaymovich, A. Das, and R. Moessner, Multifractality without fine-tuning in a Floquet quasiperiodic chain, *SciPost Phys.* **4**, 025 (2018).
- [39] T. Cadez, R. Mondaini, and P. D. Sacramento, Edge and bulk localization of Floquet topological superconductors, *Phys. Rev. B* **99**, 014301 (2019).
- [40] P. Bordia, H. Lüschen, U. Schneider, M. Knap, and I. Bloch, Periodically driving a many-body localized quantum system, *Nat. Phys.* **13**, 460 (2017).
- [41] M. Sarker, R. Ghosh, A. Sen, and K. Sengupta, Mobility edge and multifractality in a periodically driven Aubry-André model, *Phys. Rev. B* **103**, 184309 (2021).
- [42] P. T. Dumitrescu, J. G. Bohnet, J. P. Gaebler, A. Hankin, D. Hayes, A. Kumar, B. Neyenhuis, R. Vasseur, and A. C. Potter, Dynamical topological phase realized in a trapped-ion quantum simulator. *Nature* **607**, 463 (2022).
- [43] H. Jiang, L.-J. Lang, C. Yang, S.-L. Zhu, and S. Chen, Interplay of non-Hermiticity and disorder in the one-dimensional Aubry-André model, *Phys. Rev. B* **100**, 054301 (2019).
- [44] S. Longhi, Topological phase transition in non-Hermitian quasicrystals, *Phys. Rev. Lett.* **122**, 237601 (2019).
- [45] K. Kawabata, K. Shiozaki, M. Ueda, and M. Sato, Symmetry and topology in non-Hermitian physics, *Phys. Rev. X* **9**, 041015 (2019).
- [46] Y. Liu, Y. Wang, X.-J. Liu, Q. Zhou, and S. Chen, Exact mobility edges, PT-symmetry breaking, and skin effect in one-dimensional non-Hermitian quasicrystals, *Phys. Rev. B* **103**, 014203 (2021).
- [47] Y. Liu, Q. Zhou, and S. Chen, Localization transition, spectrum structure, and winding numbers for one-dimensional non-Hermitian quasicrystals, *Phys. Rev. B* **104**, 024201 (2021).
- [48] Y. Liu, Y. Wang, Z. Zheng, and S. Chen, Exact non-Hermitian mobility edges in one-dimensional quasicrystal lattice with exponentially decaying hopping and its dual lattice, *Phys. Rev. B* **103**, 134208 (2021).
- [49] Q. Lin, T. Li, L. Xiao, K. Wang, W. Yi, and P. Xue, Topological phase transitions and mobility edges in non-Hermitian quasicrystals, *Phys. Rev. Lett.* **129**, 113601 (2022).
- [50] S. Longhi, Metal-insulator phase transition in a non-Hermitian Aubry-André-Harper model, *Phys. Rev. B* **100**, 125157 (2019).
- [51] S.-Z. Li and Z. Li, Ring structure in the complex plane: A fingerprint of a non-Hermitian mobility edge, *Phys. Rev. B* **110**, L041102 (2004).
- [52] D. Peng, S. Cheng, and G. Xianlong, Power-law hopping of single particles in one-dimensional non-Hermitian quasicrystals, *Phys. Rev. B* **107**, 174205 (2023).
- [53] Q.-B. Zeng, Y.-B. Yang, and Y. Xu, Topological phases in non-Hermitian Aubry-André-Harper models. *Phys. Rev. B* **101**, 020201(R)(2020).
- [54] F. A. An, K. Padavić, E. J. Meier, S. Hegde, S. Ganeshan, J. H. Pixley, S. Vishveshwara, and B. Gadway, Interactions and mobility edges: Observing the generalized Aubry-André model, *Phys. Rev. Lett.* **126**, 040603 (2021).
- [55] G. Roati, C. D'Errico, L. Fallani, M. Fattori, C. Fort, M. Zaccanti, G. Modugno, M. Modugno, and M. Inguscio, Anderson localization of a non-interacting Bose-Einstein condensate, *Nature (London)* **453**, 895 (2008).
- [56] L. Fallani, J. E. Lye, V. Guarrera, C. Fort, and M. Inguscio, Ultracold atoms in a disordered crystal of light: Towards a Bose glass, *Phys. Rev. Lett.* **98**, 130404 (2007).
- [57] C. D'Errico, E. Lucioni, L. Tanzi, L. Gori, G. Roux, I. P. McCulloch, T. Giamarchi, M. Inguscio, and G. Modugno, Observation of a disordered bosonic insulator from weak to strong interactions, *Phys. Rev. Lett.* **113**, 095301 (2014).
- [58] M. Schreiber, S. S. Hodgman, P. Bordia, H. P. Lüschen, M. H. Fischer, R. Vosk, E. Altman, U. Schneider, and I. Bloch, Observation of many-body localization of interacting fermions in a quasirandom optical lattice, *Science* **349**, 842 (2015).
- [59] P. Bordia, H. P. Lüschen, S. S. Hodgman, M. Schreiber, I. Bloch, and U. Schneider, Coupling identical onedi-

- dimensional many-body localized systems, *Phys. Rev. Lett.* **116**, 140401 (2016).
- [60] P. Bordia, H. P. Lüschen, S. Scherg, S. Gopalakrishnan, M. Knap, U. Schneider, and I. Bloch, Probing slow relaxation and many-body localization in two-dimensional quasiperiodic systems, *Phys. Rev. X* **7**, 041047 (2017).
- [61] H. P. Lüschen, P. Bordia, S. Scherg, F. Alet, E. Altman, U. Schneider, and I. Bloch, Observation of slow dynamics near the many-body localization transition in one-dimensional quasiperiodic systems, *Phys. Rev. Lett.* **119**, 260401 (2017).
- [62] H. P. Lüschen, S. Scherg, T. Kohlert, M. Schreiber, P. Bordia, X. Li, S. D. Sarma, and I. Bloch, Single-particle mobility edge in a one-dimensional quasiperiodic optical lattice, *Phys. Rev. Lett.* **120**, 160404 (2018).
- [63] F. A. An, E. J. Meier, and B. Gadway, Engineering a fluxdependent mobility edge in disordered zigzag chains, *Phys. Rev. X* **8**, 031045 (2018).
- [64] Y. Wang, J.-H Zhang, Y. Li, J. Wu, W. Liu, F. Mei, Y. Hu, L. Xiao, J. Ma, C. Chin, and S. Jia, Observation of interactioninduced mobility edge in an atomic Aubry-André wire, *Phys. Rev. Lett.* **129**, 103401 (2022).
- [65] Y. Lahini, R. Pugatch, F. Pozzi, M. Sorel, R. Morandotti, N. Davidson, and Y. Silberberg, Observation of a localization transition in quasiperiodic photonic lattices, *Phys. Rev. Lett.* **103**, 013901 (2009).
- [66] P. Wang, Y. Zheng, X. Chen, C. Huang, Y. V. Kartashov, L. Torner, V. V. Konotop, and F. Ye, Localization and delocalization of light in photonic moire lattices, *Nature* **577**, 42 (2020).
- [67] Y. E. Kraus, Y. Lahini, Z. Ringel, M. Verbin, and O. Zilberberg, Topological states and adiabatic pumping in quasicrystals, *Phys. Rev. Lett.* **109**, 106402 (2012).
- [68] M. Verbin, O. Zilberberg, Y. E. Kraus, Y. Lahini, and Y. Silberberg, Observation of topological phase transitions in photonic quasicrystals, *Phys. Rev. Lett.* **110**, 076403 (2013).
- [69] M. Verbin, O. Zilberberg, Y. Lahini, Y. E. Kraus, and Y. Silberberg, Topological pumping over a photonic Fibonacci quasicrystal, *Phys. Rev. B* **91**, 064201 (2015).
- [70] A. D. Sinelnik, I. I. Shishkin, X. Yu, K. B. Samusev, P. A. Belov, M. F. Limonov, P. Ginzburg, and M. V. Rybin, Experimental Observation of Intrinsic Light Localization in Photonic Icosahedral Quasicrystals, *Adv. Opt. Mater.* **8**, 2001170 (2020).
- [71] P. Wang, Q. Fu, R. Peng, Y. V. Kartashov, L. Torner, V. V. Konotop, and F. Ye, Two-dimensional Thouless pumping of light in photonic moiré lattices, *Nat. Commun.* **13**, 6738 (2022).
- [72] Y. Lahini, R. Pugatch, F. Pozzi, M. Sorel, R. Morandotti, N. Davidson, and Y. Silberberg, Observation of a localization transition in quasiperiodic photonic lattices, *Phys. Rev. Lett.* **103**, 013901 (2009).
- [73] D. Tanese, E. Gurevich, F. Baboux, T. Jacqmin, A. Lemaître, E. Galopin, I. Sagnes, A. Amo, J. Bloch, and E. Akkermans, Fractal energy spectrum of a polariton gas in a Fibonacci quasiperiodic potential, *Phys. Rev. Lett.* **112**, 146404 (2014).
- [74] V. Goblot, A. Štrkalj, N. Pernet, J. L. Lado, C. Dorow, A. Lemaître, L. Le Gratiet, A. Harouri, I. Sagnes, S. Ravets, A. Amo, J. Bloch, and O. Zilberberg, Emergence of criticality through a cascade of delocalization transitions in quasiperiodic chains, *Nat. Phys.* **16**, 832 (2020).
- [75] P. Roushan et al., Spectroscopic signatures of localization with interacting photons in superconducting qubits, *Science* **358**, 6367 (2017).
- [76] H. Li, Y.-Y Wang, Y.-H Shi, K. Huang, X. Song, G.-H Liang, Z.-Y Mei, B. Zhou, H. Zhang, J.-C Zhang, S. Chen, S.-P. Zhao, Y. Tian, Z.-Y Yang, Z. Xiang, K. Xu, D. Zheng, and H. Fan, Observation of critical phase transition in a generalized Aubry-André-Harper model with superconducting circuits, *npj Quantum Inf.* **9**, 40 (2023).
- [77] See Supplemental Material for details.
- [78] L. Wang, N. Liu, S. Chen, and Y. Zhang, Quantum walks in the commensurate off-diagonal Aubry-André-Harper model. *Phys. Rev. A* **95**, 013619(2017).
- [79] Karl H. Hoffmann, and M. Schreiber, *Computational Physics: Selected Methods Simple Exercises Serious Applications*. Springer (2012).
- [80] F. Deng, X. Chen, X. Luo, W. Zhang, S. Yi, and T. Shi, Effective Potential and Superfluidity of Microwave-Shielded Polar Molecules. *Phys. Rev. Lett.* **130**, 183001 (2023).

Supplemental Material for ‘‘A Family of Self-Dual Models for One-Dimensional Quasicrystals’’

In this Supplemental Material, we provide more details on (I) The self-duality of the Hamiltonian; (II) Some exemplary applications of our scheme; (IV) Symmetry of the off-diagonal quasiperiodic models; (V) Implementation with Rydberg-atom array.

THE SELF-DUALITY OF THE HAMILTONIAN

The Hamiltonians described in Eq. (1) of the main text do not include onsite terms. Here, we consider a more general case

$$\hat{H}(a, b) = \sum_{mn} \hat{b}_m^\dagger \hat{b}_n (1 + \delta_{mn}) f_{|m-n|}(a) F_{m+n}(b), \quad (\text{S1})$$

where \hat{b}_n^\dagger (\hat{b}_n) are the creation (annihilation) operators on site n , and δ_{mn} is the Kronecker delta. The modulation functions $f_{|m-n|}(a)$ and $F_{m+n}(b)$ are related via $F_x(a) = \sum_{s=0}^{+\infty} f_s(a) \cos(\tau s \pi x)$. The models considered in the main text correspond to the special case with $f_0(a) = 0$, that is, no on-site term.

Equation (S1) can be expressed as

$$\hat{H}(a, b) = \sum_{t=0}^{+\infty} \sum_{s=0}^{+\infty} f_t(a) f_s(b) \sum_n \{ \hat{b}_n^\dagger \hat{b}_{n+t} \cos[\pi \tau s (2n + t)] + \hat{b}_n^\dagger \hat{b}_{n-t} \cos[\pi \tau s (2n - t)] \}. \quad (\text{S2})$$

We observe that

$$\begin{aligned} & \sum_n \hat{b}_n^\dagger \hat{b}_{n+t} \cos[\pi \tau s (2n + t)] \\ &= \frac{1}{2N} \sum_{nkq} \tilde{b}_k^\dagger \tilde{b}_q e^{2i\pi \tau nk} e^{-2i\pi \tau (n+t)q} (e^{i\pi \tau s (2n+t)} + e^{-i\pi \tau s (2n+t)}) \\ &= \frac{1}{2} \sum_{kq} \tilde{b}_k^\dagger \tilde{b}_q e^{-i\pi \tau t (2q-s)} \left(\frac{1}{N} \sum_n e^{2i\pi \tau n (k-q+s)} \right) \\ & \quad + \frac{1}{2} \sum_{kq} \tilde{b}_k^\dagger \tilde{b}_q e^{-i\pi \tau t (2q+s)} \left(\frac{1}{N} \sum_n e^{2i\pi \tau n (k-q-s)} \right) \\ &= \frac{1}{2} \sum_{kq} \tilde{b}_k^\dagger \tilde{b}_q (e^{-i\pi \tau t (2q-s)} \delta_{q, k+s} + e^{-i\pi \tau t (2q+s)} \delta_{q, k-s}) \\ &= \frac{1}{2} \sum_k (\tilde{b}_k^\dagger \tilde{b}_{k+s} e^{-i\pi \tau t (2k+s)} + \tilde{b}_k^\dagger \tilde{b}_{k-s} e^{-i\pi \tau t (2k-s)}). \end{aligned} \quad (\text{S3})$$

Similarly,

$$\sum_n \hat{b}_n^\dagger \hat{b}_{n-t} \cos[\pi \tau s (2n - t)] = \frac{1}{2} \sum_k (\tilde{b}_k^\dagger \tilde{b}_{k+s} e^{i\pi \tau t (2k+s)} + \tilde{b}_k^\dagger \tilde{b}_{k-s} e^{i\pi \tau t (2k-s)}). \quad (\text{S4})$$

Combining the results above, we find

$$\begin{aligned} & \sum_n \{ \hat{b}_n^\dagger \hat{b}_{n+t} \cos[\pi \tau s (2n + t)] + \hat{b}_n^\dagger \hat{b}_{n-t} \cos[\pi \tau s (2n - t)] \} \\ &= \frac{1}{2} \sum_k \tilde{b}_k^\dagger \tilde{b}_{k+s} (e^{-i\pi \tau t (2k+s)} + e^{i\pi \tau t (2k+s)}) \\ & \quad + \frac{1}{2} \sum_k \tilde{b}_k^\dagger \tilde{b}_{k-s} (e^{-i\pi \tau t (2k-s)} + e^{i\pi \tau t (2k-s)}) \\ &= \sum_k \{ \tilde{b}_k^\dagger \tilde{b}_{k+s} \cos[\pi \tau t (2k + s)] + \tilde{b}_k^\dagger \tilde{b}_{k-s} \cos[\pi \tau t (2k - s)] \}. \end{aligned} \quad (\text{S5})$$

Consequently, Eq. (S2) becomes

$$\hat{H}(a, b) = \sum_{t=0}^{+\infty} \sum_{s=0}^{+\infty} f_t(a) f_s(b) \sum_k \{ \tilde{b}_k^\dagger \tilde{b}_{k+s} \cos[\pi\tau t(2k+s)] + \tilde{b}_k^\dagger \tilde{b}_{k-s} \cos[\pi\tau t(2k-s)] \}, \quad (\text{S6})$$

which can be compactly written as

$$\hat{H}(a, b) = \sum_{k \neq l} \tilde{b}_k^\dagger \tilde{b}_l (1 + \delta_{kl}) f_{|k-l|}(b) F_{k+l}(a). \quad (\text{S7})$$

Notably, the resulting expression has the same form as $\hat{H}(b, a)$ but in the dual space representation. This implies that $\hat{H}(a, b)$ is dual to $\hat{H}(b, a)$, leading to the self-duality condition $a = b$.

SOME EXEMPLARY APPLICATIONS

In this section, we derive some exemplary self-dual models, based on our general framework.

First, we re-derive the self-dual points of the AAH model. To this end, we define a modified function $F'_x(a)$ based on $F_x(a) = \sum_{s=0}^{+\infty} f_s(a) \cos(\tau s \pi x)$ as follows

$$F'_x(a) = F_x(a) - f_0(a) = \sum_{s=1}^{+\infty} f_s(a) \cos(\tau s \pi x). \quad (\text{S8})$$

We denote the Hamiltonians constructed from $F_x(a)$ and $F'_x(a)$ as $H(a, b)$ and $H'(a, b)$, respectively. By subtracting these two Hamiltonians, we obtain a new Hamiltonian

$$\begin{aligned} \hat{H}_S(a, b) &= \hat{H}(a, b) - \hat{H}'(a, b) \\ &= 2f_0(a)f_0(b) \sum_n \hat{b}_n^\dagger \hat{b}_n + \sum_n \sum_{s=1}^{+\infty} [2f_0(a)f_s(b) \cos(2\tau s \pi n) \hat{b}_n^\dagger \hat{b}_n + f_0(b)f_s(a) (\hat{b}_{n+s}^\dagger \hat{b}_n + \hat{b}_n^\dagger \hat{b}_{n+s})]. \end{aligned} \quad (\text{S9})$$

Since $H(a, b)$ and $H'(a, b)$ are dual to $H(b, a)$ and $H'(b, a)$, respectively, it follows that $\hat{H}_S(a, b)$ is also dual to $\hat{H}_S(b, a)$. For simplicity, We omit the first term in \hat{H}_S , as it's a constant term given that $\sum_n \hat{b}_n^\dagger \hat{b}_n = 1$.

As a first example, consider the choice

$$F_x(a) = 1 + a \cos(\tau \pi x), \quad (\text{S10})$$

yields the subtracted Hamiltonian

$$\hat{H}_S(a, b) = \sum_n [2b \cos(2\tau s \pi n) \hat{b}_n^\dagger \hat{b}_n + a (\hat{b}_{n+s}^\dagger \hat{b}_n + \hat{b}_n^\dagger \hat{b}_{n+s})], \quad (\text{S11})$$

which corresponds precisely to the AAH model. The self-dual point $a = b$ matches the well-known duality condition of the AAH model.

As another example, we derive the model studied in Ref. [20]. We take

$$F_x(a) = 1 + a \sum_{s=1}^{+\infty} \frac{1}{s^p} \cos(\tau s \pi x), \quad (\text{S12})$$

where p is the parameter governs the power-law decay. This leads to the Hamiltonian

$$\hat{H}_S(a, b) = \sum_n \sum_{s=1}^{+\infty} \left[\frac{2b}{s^p} \cos(2\tau s \pi n) \hat{b}_n^\dagger \hat{b}_n + \frac{a}{s^p} (\hat{b}_{n+s}^\dagger \hat{b}_n + \hat{b}_n^\dagger \hat{b}_{n+s}) \right], \quad (\text{S13})$$

which corresponds to the model studied in Ref. [20]. Again, the condition $a = b$ consistently defines the self-dual point.

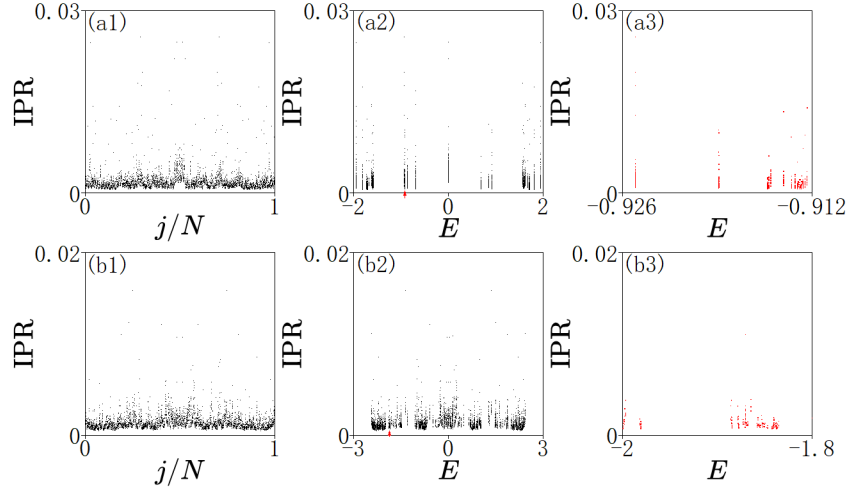


Fig S1. IPR as a function of the normalized eigenstate index j/N and eigenvalue E for the Hamiltonian with modulation $F_x(a)$ given by a square wave, shown for (a1-a3) $d = 3$ and (b1-b3) $d = 100$. (a3)(b3) Zoomed-in views of the regions indicated by red arrows in (a2) and (b2), respectively. The system size is $N = 6765$, and periodic boundary conditions are imposed in all panels.

Finally, we analyze a simple square-wave function $F_x(a)$ and its corresponding dual model. We define $F_x(a)$ as a square wave

$$F_x(a) = \begin{cases} a, & (2n - \frac{1}{2})\frac{1}{\tau} < x < (2n + \frac{1}{2})\frac{1}{\tau} \\ 0, & x = (n + \frac{1}{2})\frac{1}{\tau} \\ -a, & (2n + \frac{1}{2})\frac{1}{\tau} < x < (2n + \frac{3}{2})\frac{1}{\tau} \end{cases}, n \in \mathbb{Z} \quad (\text{S14})$$

and this function can also be written in its Fourier expansion as

$$F_x(a) = \sum_{s=1}^{+\infty} a \frac{4 \sin(\frac{\pi s}{2})}{\pi s} \cos(\tau s \pi x). \quad (\text{S15})$$

The corresponding Hamiltonian is

$$\hat{H}(a, b) = \sum_{m \neq n} \hat{b}_m^\dagger \hat{b}_n a \frac{4 \sin(\frac{\pi|m-n|}{2})}{\pi|m-n|} \sum_{s=1}^{+\infty} b \frac{4 \sin(\frac{\pi s}{2})}{\pi s} \cos[\tau s \pi(m+n)]. \quad (\text{S16})$$

Notably, Eq. (S16) remains invariant under the dual transformation, indicating that all eigenstates of this model are critical.

For a truncated version of the square wave, we define:

$$F'_x(a) = \sum_{s=1}^d \frac{4a \sin(\frac{\pi s}{2})}{\pi s} \cos(\tau s \pi x), \quad (\text{S17})$$

$$\hat{H}'(a, b) = \sum_{1 \leq |m-n| \leq d} \hat{b}_m^\dagger \hat{b}_n \frac{4a \sin(\frac{\pi|m-n|}{2})}{\pi|m-n|} F'_{m+n}(b). \quad (\text{S18})$$

The IPR distributions for different truncation distances d as a function of the normalized eigenstate index j/N and eigenvalue E are shown in Fig. S1. We observe that the eigenstates cluster into narrow bands, exhibiting pronounced fine structures across the spectrum.

SYMMETRY OF THE OFF-DIAGONAL QUASIPERIODIC MODELS

Off-diagonal quasiperiodic models with nearest-neighbor hopping terms exhibit a distinct symmetry in their eigenvalue and eigenstates. We consider the Hamiltonian of the form

$$\hat{H} = \sum_n h_n (\hat{b}_n^\dagger \hat{b}_{n+1} + \hat{b}_{n+1}^\dagger \hat{b}_n), \quad (\text{S19})$$

where \hat{b}^\dagger and \hat{b} are creation and annihilation operators at site n , and h_n are the hopping coefficients. The corresponding eigenequation is

$$h_{n-1}\phi_{n-1} + h_n\phi_{n+1} = E\phi_n, \quad (\text{S20})$$

where ϕ_n represents the n th component of ϕ . Now define a new state φ by

$$\varphi_n = (-1)^n \phi_n. \quad (\text{S21})$$

Substituting this into Eq. (S20), we have

$$h_{n-1}\varphi_{n-1} + h_n\varphi_{n+1} = -E\varphi_n. \quad (\text{S22})$$

Thus, φ_n is also an eigenstate of the Hamiltonian, but with energy $-E$. This indicates that for every eigenstate with energy E , there exists a corresponding eigenstate with energy $-E$ that has the same spatial profile, apart from a staggered sign alternation on odd (or even) lattice sites. This establishes a spectral symmetry about $E = 0$.

IMPLEMENTATION WITH RYDBERG-ATOM ARRAY

Consider an one-dimensional Rydberg ^{87}Rb atom chain, the total Hamiltonian governing the system is given by [80]

$$\hat{H} = \sum_n \hat{H}_{0,n} + \sum_n \hat{H}_{in,n} + \sum_{m < n} \hat{H}_{ddi,mn}, \quad (\text{S23})$$

where $\hat{H}_{0,n}$ describes the internal states of the n -th atom, $\hat{H}_{in,n}$ represents the interaction between the atom and the microwave field, and $\hat{H}_{ddi,mn}$ accounts for the dipole-dipole interaction between atoms m -th and n -th atoms, which depends on their separation distance. The internal-state space of the atom on the n th site includes the Rydberg states $|60S_{1/2}, m_j = 1/2\rangle$, denoted as $|0\rangle_n$, as well as $|60P_{3/2}, m_j = 3/2\rangle$ and $|60P_{3/2}, m_j = -1/2\rangle$, denoted as $|+\rangle_n$ and $|-\rangle_n$, respectively. By applying a magnetic field gradient, a site-dependent energy splitting of $2\Delta_n$ is introduced between the states $|+\rangle_n$ and $|-\rangle_n$. These two states are additionally coupled by site-dependent microwave fields with Rabi frequency Ω_n . Note that the values of the Ω_n and Δ_n are specified below.

Each term in Eq.(S23) can be expressed as

$$\hat{H}_{0,n} = E_0|0\rangle_n\langle 0|_n + E_1(|+\rangle_n\langle +|_n + |-\rangle_n\langle -|_n), \quad (\text{S24})$$

$$\hat{H}_{in,n} = \Delta_n(|+\rangle_n\langle +|_n - |-\rangle_n\langle -|_n) + \Omega_n(|+\rangle_n\langle -|_n + |-\rangle_n\langle +|_n), \quad (\text{S25})$$

$$\hat{H}_{ddi,mn} = -8\sqrt{\frac{2}{15}}\pi^{\frac{3}{2}}\frac{d^2}{4\pi\epsilon_0 D_{mn}^3} \sum_{M=-2}^2 Y_{2,M}^*(\theta, \varphi) \hat{\Sigma}_{2,M;mn}. \quad (\text{S26})$$

Here d is the dipole matrix element of the Rydberg states and D_{mn} is the separation between the m th and n th atoms. $Y_{2,M}(\theta, \varphi)$ are the spherical harmonics with (θ, φ) the spherical polar angles determined by the orientation of the chain. The operator $\hat{\Sigma}_{2,M}$ is defined as

$$\hat{\Sigma}_{2,0;mn} = \frac{1}{\sqrt{6}}(\hat{d}_m^+ \otimes \hat{d}_n^- + \hat{d}_m^- \otimes \hat{d}_n^+ + 2\hat{d}_m^0 \otimes \hat{d}_n^0), \quad (\text{S27})$$

$$\hat{\Sigma}_{2,\pm 1;mn} = \hat{d}_m^\pm \otimes \hat{d}_n^0 + \hat{d}_m^0 \otimes \hat{d}_n^\pm, \quad \hat{\Sigma}_{2,\pm 2;mn} = \hat{d}_m^\pm \otimes \hat{d}_n^\pm, \quad (\text{S28})$$

with

$$\hat{d}_n^0 = 0, \quad (\text{S29})$$

$$\hat{d}_n^+ = \frac{1}{\sqrt{4\pi}}(|+\rangle_n \langle 0|_n - |0\rangle_n \langle -|_n), \hat{d}_n^- = -(\hat{d}_n^+)^\dagger. \quad (\text{S30})$$

In the basis $\{|+\rangle_n, |-\rangle_n\}$, $\hat{H}_{in,n}$ can be expressed in the Bloch form as

$$\hat{H}_{in,n} = \mathbf{n}_{in,n} \cdot \boldsymbol{\sigma}, \quad (\text{S31})$$

where $\mathbf{n}_{in,n} = (\Omega_n, 0, \Delta_n)$, and $\boldsymbol{\sigma} = (\sigma_x, \sigma_y, \sigma_z)$ is the Pauli matrix vector. The eigenstates of $\hat{H}_{in,n}$ are then

$$|\xi_+\rangle_n = \begin{pmatrix} \cos \frac{\alpha_n}{2} \\ \sin \frac{\alpha_n}{2} \end{pmatrix}, |\xi_-\rangle_n = \begin{pmatrix} -\sin \frac{\alpha_n}{2} \\ \cos \frac{\alpha_n}{2} \end{pmatrix}, \quad (\text{S32})$$

with corresponding energies $E_{\xi_{\pm},n} = \pm \sqrt{\Delta_n^2 + \Omega_n^2}$, and $\cos \alpha_n = \frac{\Delta_n}{\sqrt{\Delta_n^2 + \Omega_n^2}}$, $\sin \alpha_n = \frac{\Omega_n}{\sqrt{\Delta_n^2 + \Omega_n^2}}$.

We require that $\sqrt{\Delta_n^2 + \Omega_n^2}$ should be site-independent, and denote it as ΔE . Furthermore, we impose the condition

$$E_0 \ll E_1 - \Delta E \ll E_1 + \Delta E, \quad (\text{S33})$$

which means that the energy differences are much larger than the characteristic strength of the dipole-dipole interaction. In the interaction picture, we then have

$$\hat{H}_I = \hat{U}^\dagger \sum_{m < n} \hat{H}_{ddi,mn} \hat{U}, \quad (\text{S34})$$

where

$$\hat{U} = \exp[-it(\sum_n \hat{H}_{0,n} + \sum_n \hat{H}_{in,n})]. \quad (\text{S35})$$

For convenience, we define

$$\hat{H}_{I,mn} = \hat{U}_{mn}^\dagger \hat{H}_{ddi,mn} \hat{U}_{mn}, \quad (\text{S36})$$

where

$$\hat{U}_{mn} = \exp[-it(\hat{H}_{0,m} + \hat{H}_{in,m} + \hat{H}_{0,n} + \hat{H}_{in,n})]. \quad (\text{S37})$$

Applying the rotating-wave approximation, Eq. (S36) simplifies to

$$\hat{H}_{I,mn} = J_{\xi_+,mn} \hat{b}_{\xi_+,m}^\dagger \hat{b}_{\xi_+,n} + J_{\xi_+,nm} \hat{b}_{\xi_+,n}^\dagger \hat{b}_{\xi_+,m} + J_{\xi_-,mn} \hat{b}_{\xi_-,m}^\dagger \hat{b}_{\xi_-,n} + J_{\xi_-,nm} \hat{b}_{\xi_-,n}^\dagger \hat{b}_{\xi_-,m}, \quad (\text{S38})$$

where $\hat{b}_{\xi_+,n}^\dagger = |\xi_+\rangle_n \langle 0|_n$, $\hat{b}_{\xi_-,n}^\dagger = |\xi_-\rangle_n \langle 0|_n$, and $J_{\xi_+,mn}$ and $J_{\xi_-,mn}$ are the corresponding coupling coefficients. Focusing on the single-excitation subspace where only $|\xi_+\rangle$ is populated, the effective Hamiltonian reduces to a single-particle hopping model

$$\hat{H}_I = \sum_{m \neq n} J_{\xi_+,mn} \hat{b}_{\xi_+,m}^\dagger \hat{b}_{\xi_+,n}, \quad (\text{S39})$$

with

$$J_{\xi_+,mn} = \frac{1}{|m-n|^3} \left(\cos \frac{\alpha_m - \alpha_n}{2} Y_{20} + \sqrt{6} \cos \frac{\alpha_m}{2} \sin \frac{\alpha_n}{2} Y_{2-2} + \sqrt{6} \cos \frac{\alpha_n}{2} \sin \frac{\alpha_m}{2} Y_{22} \right). \quad (\text{S40})$$

By adjusting the relative orientation between the Rydberg atom chain and the dipole coordinate system, we set $Y_{20} = 0$ and $Y_{2-2} = Y_{22}$. Further, by choosing the phase $\alpha_n = 2\pi\tau n + \frac{\pi}{2}$, the Hamiltonian reduces to

$$\hat{H}_{\xi_{\pm}} = A \sum_{m \neq n} \frac{\cos[\pi\tau(m+n)]}{|m-n|^3} \hat{b}_{\xi_+,m}^\dagger \hat{b}_{\xi_+,n}, \quad (\text{S41})$$

where $A = \frac{d^2}{12\pi\epsilon_0}$. Note that the phase condition $\alpha_n = 2\pi\tau n + \frac{\pi}{2}$, as well as the requirement $\Delta_n^2 + \Omega_n^2 = \text{constant}$, impose the constraint on the choice of Δ_n and Ω_n .